

DUAL-BAND, DUAL-POLARIZED FOUR PORT MIMO ANTENNA FOR FIFTH-GENERATION COMPACT SMARTPHONES

J. Vaswani* and A. Agarwal

Electronics and Communication Engineering Department, Sangam University, Bhilwara, India
jitendra2104@gmail.com

ABSTRACT

This paper presents a four-port dual-polarized, dual-band MIMO antenna system for Fifth Generation (5G) compact phones, particularly smartphones and WLAN devices. The dual-band encompasses sub-6 GHz bands with center frequencies at 3.6 GHz and 5.5 GHz. The paper elucidates the design of the proposed antenna, along with the simulation and the experimental results. The design has two dual-band dual-polarized slot radiators placed on diagonally opposite corners of the substrate without disturbing the antenna's design symmetry. The square slot radiators are etched into the ground plane fed with two antenna feeds placed perpendicular to each other, which makes the antenna radiate in two different directions with different polarizations. The isolation between the adjunct microstrip feeding ports is improved by 3 dB by placing a thin rectangular patch diagonally between the feedlines. The obtained 6dB bandwidth of the antenna is 400 MHz (3.4 - 3.8 GHz) and 600 MHz (5.3 - 5.9 GHz), which covers the desired 5G and WLAN bands. This paper also depicts the antenna ports excited in the sequential mode and in simultaneous mode with different combinations of phases to get beam-forming, which is an essential feature for any 5G antenna. The proposed antenna has good gain, directivity, efficiency, and envelope correlation coefficient. The simulation and fabrication results are in good agreement.

Keywords: 5G, Diversity Gain, Dual-band, Dual-polarization, ECC, MIMO

1. Introduction

The hunger for data speeds is increasing day by day, and mobile communication technology is getting upgraded, 2G to 4G phones are currently available to all of us, and 5G phones will be reaching the market soon. Smartphones with a touchscreen are prevalent but costly and fragile. People who are habitual of using phones with a keypad make it very difficult for them to switch to a smartphone with a touchscreen. They still prefer to use phones with a rugged, compact, cost-effective, and familiar keypad. This type of phone was made popular in India, only the technology changed, but the look and size remain the same. One can expect that after the 5G services are launched, mobile phone designers will design a similar smartphone with a keypad. International Telecommunication Union (ITU) declared the 3.4-3.6 GHz, 5-6 GHz (i.e., sub-6 GHz band), 24.25-27.5 GHz band, 37-40.5 GHz band, and 66-76 GHz band (mm-wave) for 5G communication. (Marcus, 2015)

In (Liu et al., 2017), the authors have reviewed 5G antennas and emphasized that 5G antennas should operate on multiple frequencies and

multiple polarizations. The gain of the antennas should be high, and one can increase it by using parasitic cells. A polarization reconfigurable dipole antenna working in the frequency range of 5G Wi-Fi (5.07 to 5.95 GHz) is presented. The antenna can switch the polarization between the linearly polarized and the circularly polarized states with a gain close to 8.2 dBi with an efficiency of nearly 85% (Ge et al., 2017). A 4-port MIMO antenna design is proposed that focuses on the sub-6 GHz of 5G wireless applications. The circular shape of the antenna's ground plane is the outcome of the merger of four wideband antennas units, which leads to isolation among the four ports of the antenna (Saxena et al., 2018). A miniaturized (10.5×14.5 mm²) dual-band (2.5-2.7 GHz and 3.4 to 3.8 GHz, measured with the reflection coefficient <6dB) antenna array for 5G handsets was placed on 120x50 mm² FR-4 substrate (KHOUMA et al., 2018). A circular polarization (RHCP and LHCP) reconfigurable antenna with two PIN diode switches was also proposed for the 5G communication that resonates at 3.4 GHz, with a gain of 4.8 dBi. The antenna was fabricated on an FR-4

substrate.(Abdullah et al., 2018) A hybrid antenna module with four MIMO chip antenna was discussed that operates at 2.4 GHz ISM band and 27 GHz to 29 GHz 5G frequency band(Kahng et al., 2017). A dual-band 2x2 MIMO antenna was presented that supported 3.3 - 3.6 and 4.5 - 5 GHz in China for 5G mobile communication and achieved over 85% efficiency with isolation > 17 dB at both bands(Zhu et al., 2017). In another research article, a four-element MIMO antenna is implied for a sub-6 GHz band of 5G services. It also has split-ring resonators for getting multi-band performance with a very low value of ECC(Sarkar & Srivastava, 2018). A dual-polarized 8-element design on an FR-4 substrate is proposed with squared ring slot radiators for improved isolation between the adjunct antenna feeds. SAR function for user-hand and user-head is also studied and is proposed as a strong candidate for 5G mobile terminals(Parchin et al., 2019). In this article, a multi-band antenna covering 4G and 5G bands is proposed, and user-impact investigations are also performed. It is a MIMO designed on FR-4 substrate with double elements slot radiators with good gain and efficiency(Ojaroudi Parchin et al., 2019). A double slot four-port antenna is put forward by the authors in (J Vaswani & Agarwal, 2020) in which each of the antenna elements is placed at four corners of the square substrate and offers good gain and efficiency. Another dual-band, dual-polarized two-element slot antenna was discussed in (Jitendra Vaswani & Agarwal, 2021) having antenna gain of more than 2 dB, radiation efficiency of more than 60 percent, and had bi-directional radiation pattern.

The research gaps observed are as follows. In (Ojaroudi Parchin et al., 2019), the four antennas are placed at all four corners of the substrate, taking more space and leaving less space for other circuits. It was proposed to place the two antennas in proximity, but the mutual coupling between the adjacent antenna

elements needed investigation. In this paper, the mutual coupling between the adjacent antenna has been investigated and improved by using a thin rectangular patch between the feedlines. Another observation is that in all the antenna mentioned above designs for 5G communication systems; the researchers are designing antennas to reduce the size or designing antennas for smartphones with touchscreen whose PCB and display size is around 5 inches or more. However, for countries like India, compact smartphones with keypads have never lost their importance and are still very popular in India because of their low price, compactness, rugged body, and ease of usage. These phones available in India are GSM or LTE compatible phones. Wi-Fi hotspot is not supported on most of these phones. Considering these facts, a dual-band (3.4-3.8 GHz and 5.3 to 5.9 GHz), dual-polarized MIMO antenna is proposed for fifth-generation smartphones that will provide access to 5G services and also to Wi-Max services. The proposed antenna is designed on FR-4 substrate to work with compact smartphones, making it very affordable and application-specific. The antenna has a radiation efficiency of more than 65%, optimal IEEE gain ranging from 2.26 to 3.04 dBi in the 3.6 GHz band, 2.41 to 3.32 dBi in the 5.5 GHz band, and high diversity gain when used as a MIMO antenna. The simulation results are backed by the laboratory measurements for the proposed antenna and are in good agreement.

2. Antenna Design

Figure 1(a) shows the 4-element MIMO antenna configuration advocated and fabricated on the FR-4, an epoxy substrate that is very affordable and generously available. The dielectric constant of the same (ϵ_r) is 4.4 and loss tangent ($\tan\delta$) is 0.002. Its dimensions are $100\text{mm} \times 40\text{mm} \times 1.6\text{mm}$ with a copper thickness of 0.035mm. The proposed antenna comprises two feed elements and a parasitic patch, placed in diagonally opposite corners of

a substrate. The two square ring slots are engraved in the ground plane at the two diagonally opposite corners of the board, as shown in **Figure 1(a)**. These dimensions of the slots are responsible for the resonating frequency of the antenna. The antenna design

parameters for the feedlines and isolation patch in the front side of the antenna are shown in **Figure 1 (b)**, and the radiating slots on the backside of the antenna are shown in **Figure 1 (c)**.

Table 1. Optimized Design Parameters

Parameter	Ws	Ls	Lf	Wf	Li	Wi	W1	W2	W3	W4
Value (mm)	100	40	11.75	3	10.95	0.75	14	13.25	9.45	8.7

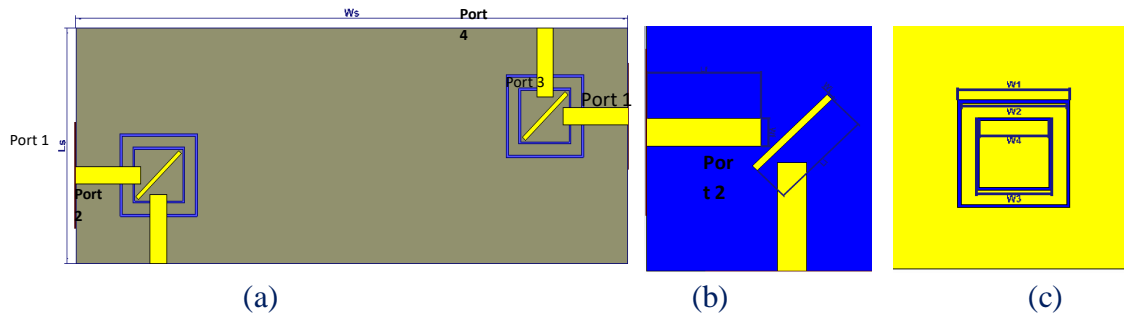


Figure 1: (a) Transparent view of the 4-port MIMO antenna configuration, (b) Front View of the unit cell (c) Back View of the unit cell for the proposed antenna

The optimized design parameter values are depicted in **Table 1**. The length of the outer and inner slots is 14 mm and 9.45 mm, while both the slots' width is 0.375 mm. The feed element is connected to a 50-Ω microstrip transmission line. The resonant frequency of the proposed antenna is inversely proportional

to slot length, so the placement and length of the slot are carefully optimized to get the antenna resonating at the desired frequencies. The outer slot makes the antenna resonate at 3.6 GHz, and the inner slot makes the antenna resonate at 5.5 GHz.

3. Results and Discussion

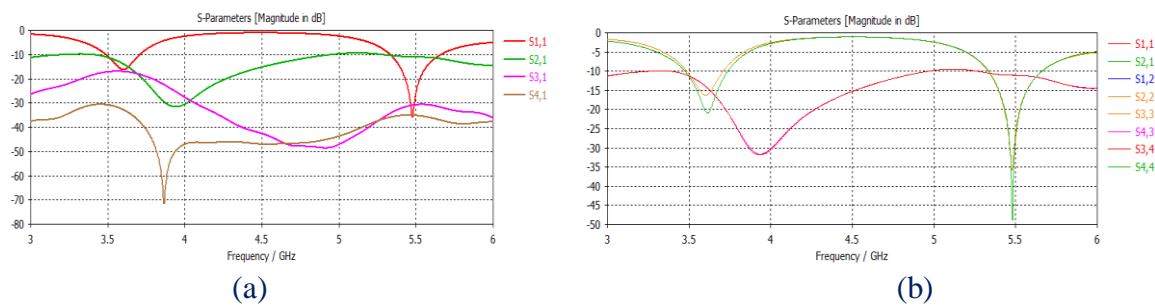


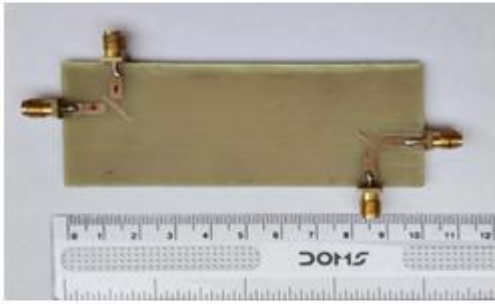
Figure 2: (a) Simulated S-Parameters for the Port 1, (b) Simulated S-Parameters for all ports with sequential excitation for the proposed antenna

Error! Reference source not found. (a) shows the simulated S-parameter results for port 1. The simulated bandwidth of the antenna is 400 MHz at 3.6 GHz and 600 MHz at 5.5 GHz. The mutual coupling between antenna 1 and antenna 2 is less than -10 dB, for antenna 1 and antenna 3 is less than -16 dB and less than -30 dB between antenna 1 and antenna 4. The

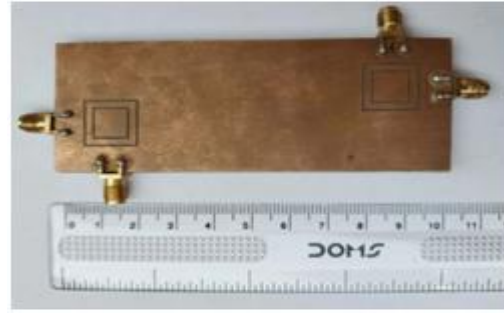
isolation amid port 1 and port 4, (S-4,1) is more than the isolation amid port 1 and port 3(S-3,1) because of the distance amid feed elements and perpendicular orientation of the feed elements with respect to each other. Isolation of 10dB is acceptable as mobile phone antennas, return loss of more than 6dB is accepted in many cases. So, there is sufficient

isolation between the antenna elements. **Error! Reference source not found.** (b) shows the individual S-parameters for all four ports (1-4)

of the antenna. The results are almost identical for port 1 and port 3 and port 2 and port 4 as they are symmetrical.



(a)



(b)

Figure 3: (a) Front and (b) Back of the Proposed Antenna after fabrication

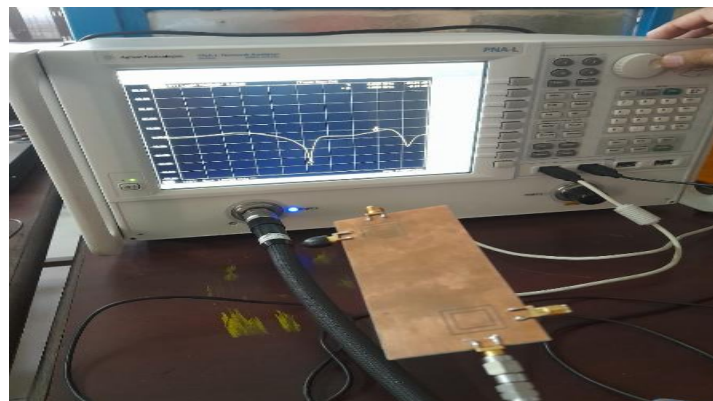


Figure 4: Proposed Antenna for S-Parameters Measurement

Figure 3 shows the antenna fabricated on FR-4 substrate. **Figure 4** shows the proposed antenna in the antenna testing lab for S-Parameter measurements with the Keysight PNA-L Microwave Network Analyser, model number N5234A that can do measurements up to the frequency of 43.5 GHz.



Figure 5: Proposed Antenna in Anechoic Chamber

Figure 5 the same proposed for radiation pattern measurement in the RF anechoic chamber. The horn antenna used in the anechoic chamber is R&S®HF907, which is a

linearly polarized, double-ridged waveguide horn antenna that operated in the frequency range up to 18 GHz

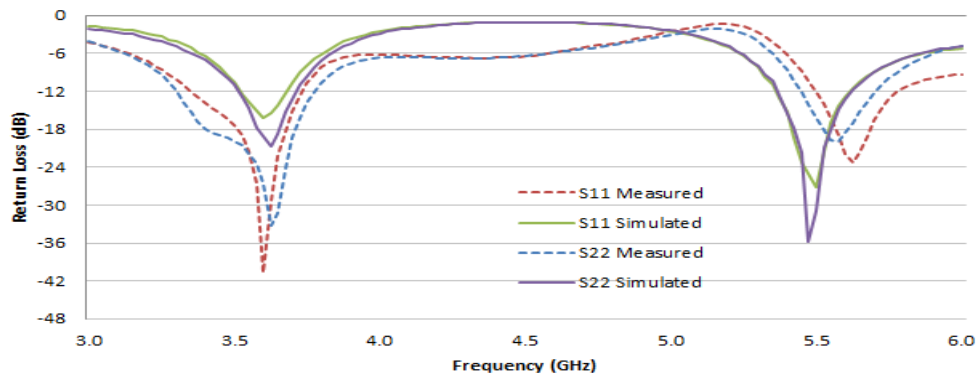


Figure 6: Simulated and Measured S-Parameters of the Proposed Antenna

The simulated and measured values of S11 are plotted and shown in Figure 6 showing the resemblance between the simulation and experimental results. The 3.6 GHz band is well aligned and there is a slight right shift of the 5.5 GHz band of antenna operation that may be due to the slight variation in dimension of the inner slot of the fabricated antenna. These variations can be dealt with by following a more accurate antenna fabrication procedure. The variation of operating frequencies with the change in the slot length (i.e., W1 and W3) is simulated, and the results are as depicted in

Figure 7. It is detected that the operating frequency is inversely proportional to the slot length, and both operating frequencies are almost independent of each other, i.e., one can shift any of the frequencies without affecting the other one. Further, it can be easily noticed that lower operating frequency varies with outer slot length (W1) and higher frequency varies with variation in inner slot length (W3). So the antenna operating frequencies are independent of each other and can be varied individually

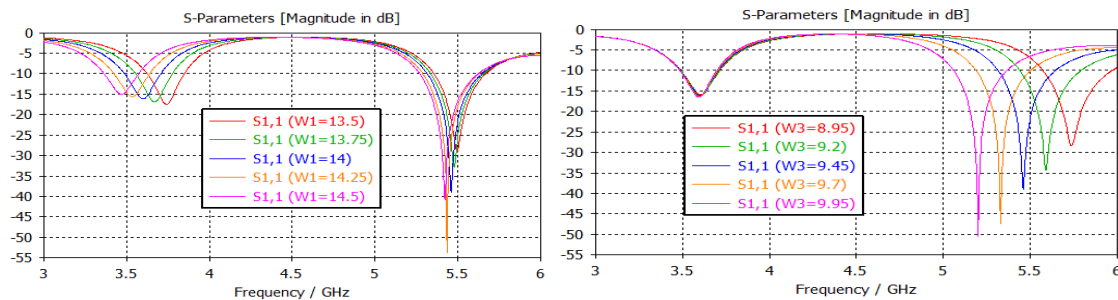


Figure 7: Simulated variation of resonant frequency with Outer and Inner Slot Length (W1 and W3) respectively for the proposed antenna

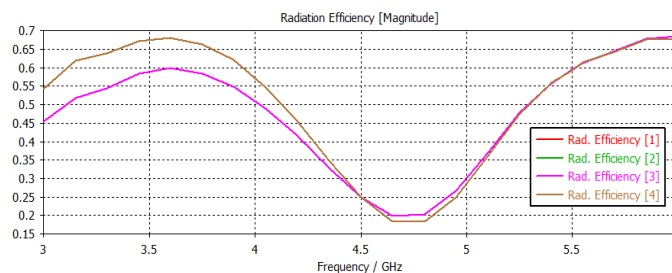


Figure 8: Simulated Radiation Efficiency for the proposed antenna for all ports

The radiation efficiencies for all the four ports of the above-discussed antenna are shown in Figure 8. The radiation efficiency is around

65% for port 2 and port 4 and 60% for port 1 and port3. So, it is more than 50% in both bands of operation for all four ports, which is

more than the theoretical requirement for the 5G mobile antennas.

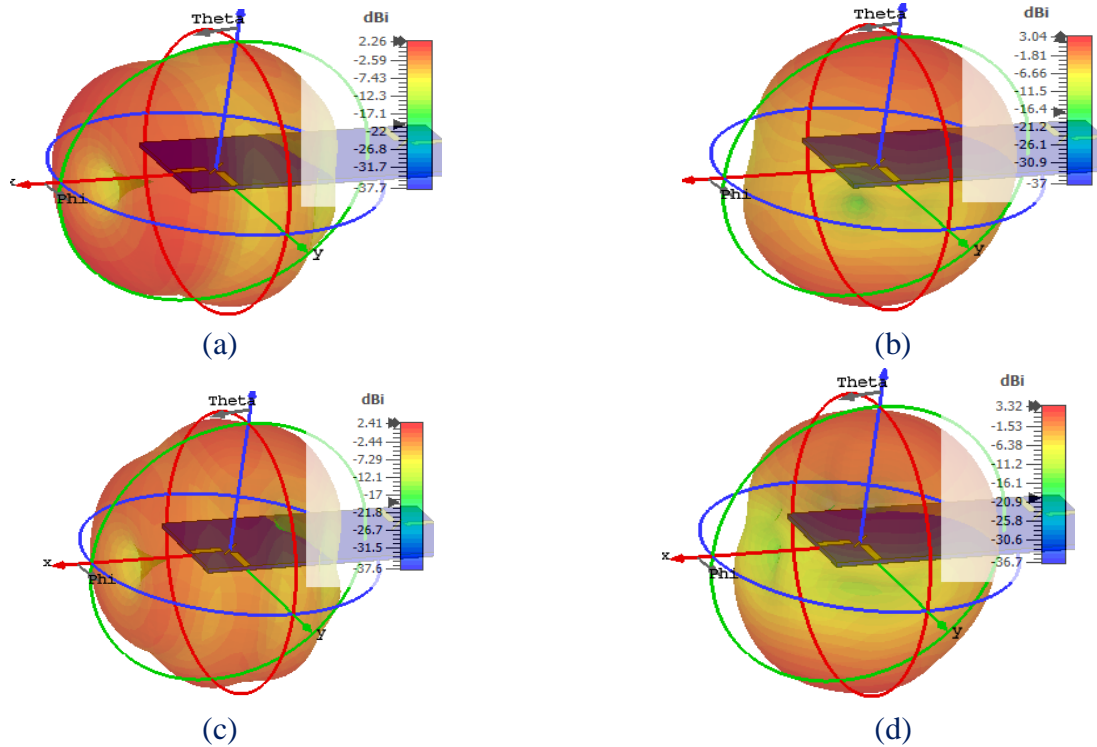
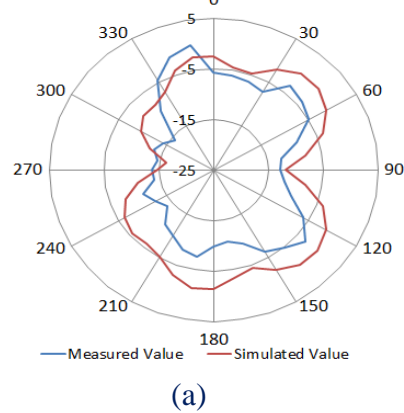


Figure 9: Simulated 3D radiation pattern for the proposed antenna (a) Port 1 at 3.6 GHz (b) Port 2 at 3.6 GHz, (c) Port 1 at 5.5 GHz (d) Port 2 at 5.5 GHz

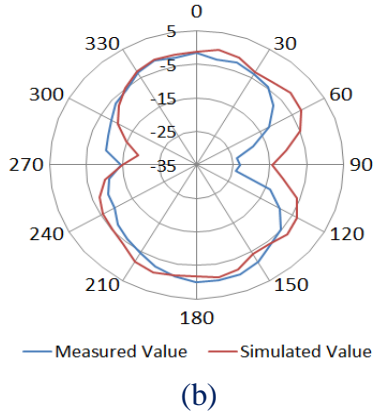
The IEEE gain is also computed for all antenna ports at both operating frequencies by exciting each port sequentially and terminating all other ports with the matched impedance. The 3D radiation patterns are shown in Figure 9. The simulated gain for the antenna ranges from 2.26 dB to 3.04 dB at 3.6 GHz and 2.41 dB to 3.32 dB at 5.5 GHz. From the 3D radiation pattern, one can notice the direction

of maximum radiation from each port of the antenna separately. Port 1 and port 2 is symmetrical to port 3 and port 4 respectively, so the results obtained are also identical for them. For port 1, the direction of maximum radiation is inclined at around 45 degrees to the plane of antenna and for port 2 the direction of maximum radiation is perpendicular to the plane of antenna.

Simulated v/s Measured 2D Radiation Pattern for Antenna Port 1 at 3.6 GHz



Simulated v/s Measured 2D Radiation Pattern for Antenna Port 1 at 5.5 GHz



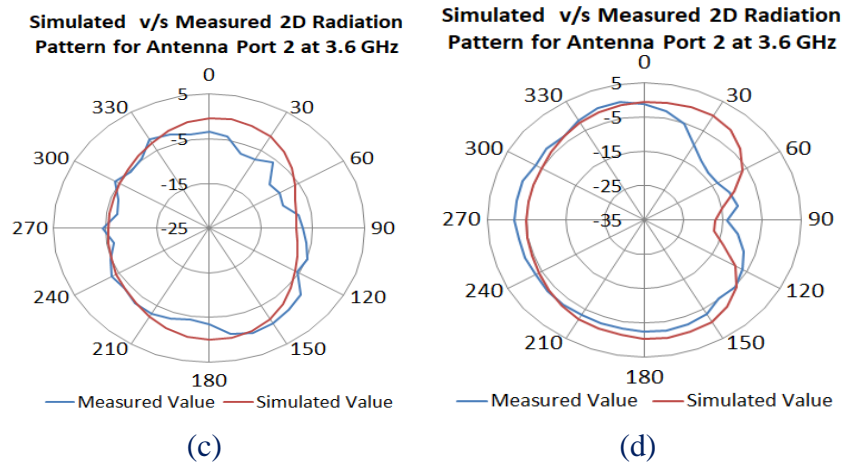


Figure 10: Simulated v/s Measured Polar plot of radiation pattern for the proposed antenna (a) Port 1 at 3.6 GHz (b) Port 2 at 3.6 GHz, (c) Port 1 at 5.5 GHz (d) Port 2 at 5.5 GHz

The same can be verified from Figure 10, which shows the simulated v/s measured polar plot of radiation pattern for the proposed antenna for port 1 and port 2 at both operating frequencies of the proposed antenna. So, while holding the phone close to the head, the mobile

would use port 1 and/or port 3 for radiating and receiving signals, and when used in handheld mode, it could use port 2 and/or port 4 for communicating. In this manner, all ports can be used for communication as per the holding position of the mobile phone.

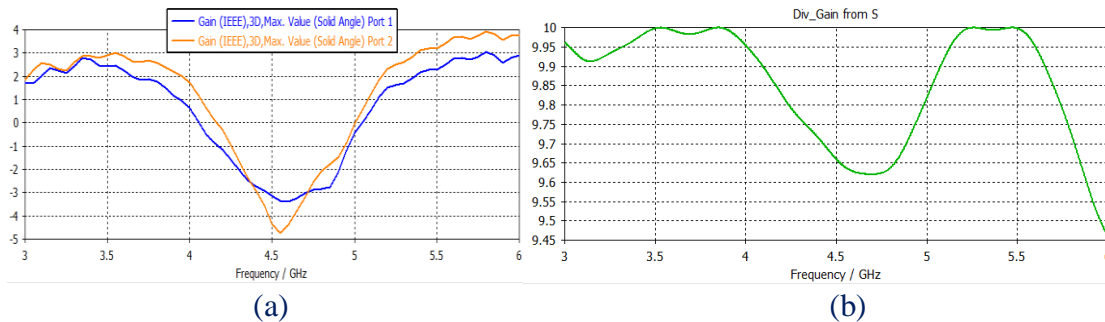


Figure 11: (a) Simulated Antenna Gain v/s Frequency for the proposed antenna for Port 1 and Port 2 (b) Variation of Simulated Diversity Gain with Frequency for the proposed antenna

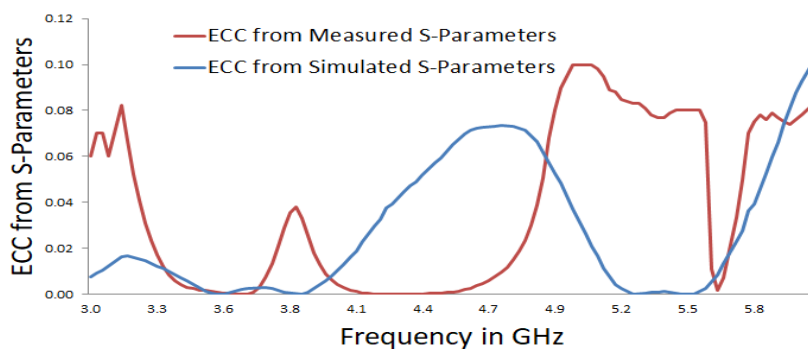


Figure 12: Simulated ECC v/s Measured ECC for the proposed antenna

The variation of gain with frequency from 3 GHz to 6 GHz is also shown in Figure 11 (a). The value of gain varies between 2 to 3 dB for both the operating bands and even crosses 3 dB for port 2 at 3.6 GHz. Another critical

parameter for the MIMO antenna is the diversity gain, which is around 10 dB in the 3.6 GHz band and more than 9.75 dB in the 5.5 GHz band, as shown in Figure 11 (b). The simulated value of diversity gain for the

proposed antenna is much more than the threshold value of 8 dB for any MIMO antenna.

Figure 12 shows the simulated envelope correlation coefficient (ECC) is well below 0.01 in 3.4 GHz to 4 GHz and for 5.2 GHz to

5.6 GHz, then it rises to 0.05 for 5.8 GHz but still less than 10% of the threshold value of 0.5. Measured ECC is below 0.02 in 3.6 GHz band and less than 0.1 in 5.5 GHz band. Both simulated and measured ECC indicates good isolation amid the antenna elements.

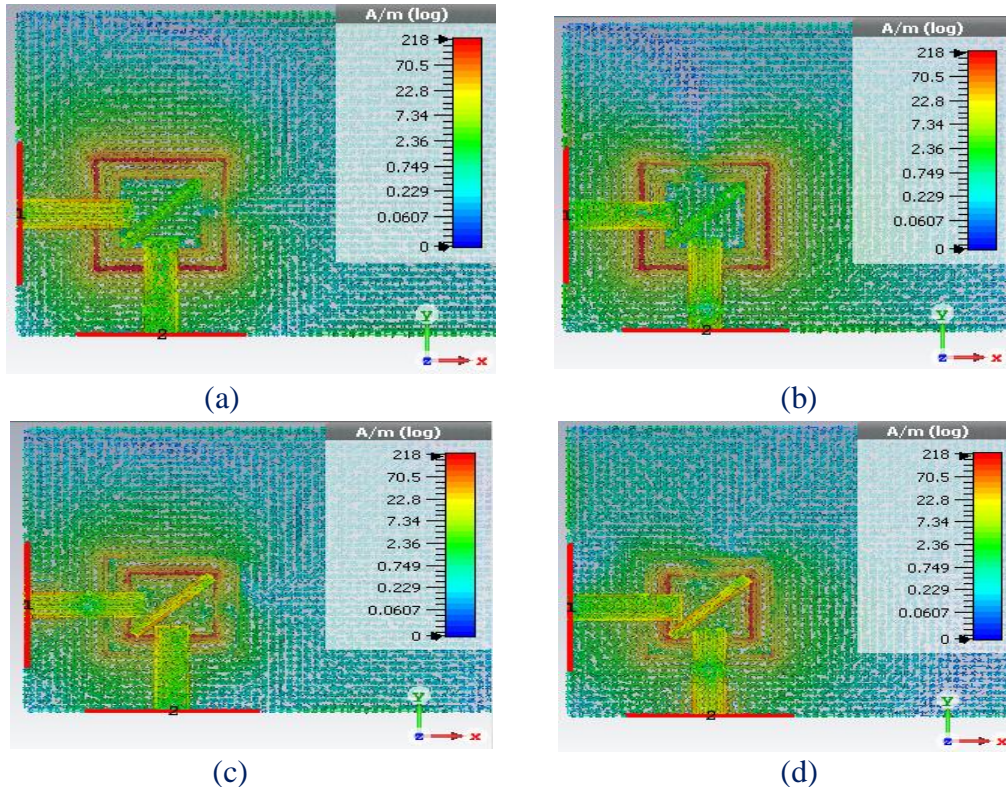


Figure 13: Distribution of Surface Current Vector for the proposed antenna (a) Port 1&3 at 3.6 GHz (b) Port 2 & 4 at 3.6 GHz (c) Port 1&3 at 5.5 GHz (d) Port 2 & 4 at 5.5 GHz

By carefully observing the surface current distribution of the antenna for both frequencies in Figure 13, it can be noticed that the outer slot is responsible for resonance at 3.6 GHz as it shows a higher current density for 3.6 GHz, and the inner slot is responsible for resonance at 5.5 GHz as the inner slot has a higher current for 5.5 GHz. Further, the rectangular parasitic patch placed diagonally increases isolation by 3 dB between the two antenna

elements at 5.5 GHz. It is observed from the surface current distribution pattern that the current density gets increased around the parasitic patch when the antenna is operating at a 5.5 GHz band. The same can be verified by comparing the s-parameters for both the designs from Figure 14. Further, the return loss also gets improved at the 5.5 GHz by more than 20 dB, and gain also gets improved by 0.15 dB.

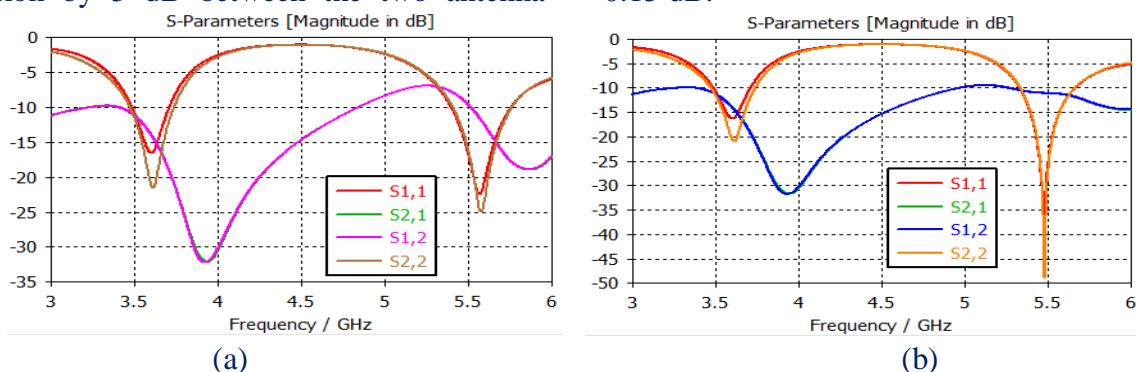


Figure 14: Simulated S-Parameters Results for the proposed antenna (a) Without Parasitic Patch (b) With Parasitic Patch

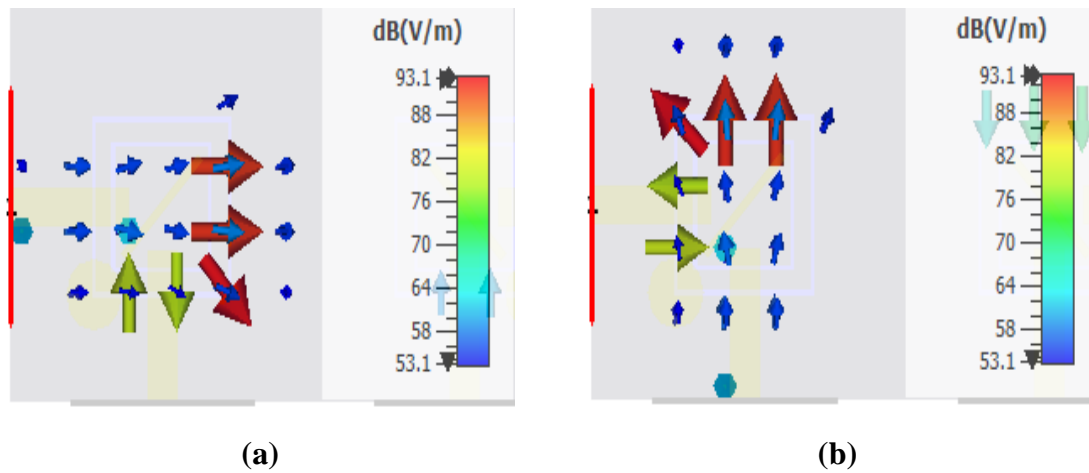


Figure 15: (a) Electric Field for Port 1 at 3.6 GHz (b) Electric Field for Port 2 at 3.6 GHz

The feed elements are placed diagonally symmetrical to each other, and each element is generating the linearly polarized wave individually. The polarization type of antenna is horizontal or vertical, depending on the relative excitation of the antenna port by the excitation source; hence, the antenna is dual-polarized and can communicate effectively in any orientation of the mobile phone. The orientation of the electric field with the excitation of the antenna port is shown in Figure 15.

Table 2 presents a comparison of fundamental properties of 5G antennas reported in the literature from (Saxena et al., 2018) to (Ojaroudi Parchin et al., 2019) with the proposed 5G antenna. It shows the antenna’s performance is at par with the reported antennas in terms of bandwidth, gain, efficiency, overall size, isolation, and ECC. Further, the proposed has ample space for placement of other components of mobile user equipment, which is not considered in the reported literature.

Table 2. Comparison between reported and proposed 5G antennas

Reference	Ports	Bandwidth (GHz)	Gain (dBi)	Efficiency (%)	Overall Size (mm ²)	Isolation (dB)	ECC
(Saxena et al., 2018)	4	3.4–3.8	4.2	–	50 × 50	12	<0.09
(KHOUM A et al., 2018)	2	2.5–2.7 3.4–3.8	–	60–76 70–82	120 × 50	11.5	–
(Zhu et al., 2017)	2	3.3–3.6 4.5–5.0	–	94 86	40 × 40	17	<0.02
(Sarkar & Srivastava, 2018)	4	3.1–3.2 3.6–4.0	1.79 2.39	58–67	60 × 60	20 17	<0.1
(Ojaroudi Parchin et al., 2019)	4	2.5–2.8 3.4–4.0 4.9–5.7	2–3	64–75 73–76 69–75	75 × 150	17	<0.05
Proposed	4	3.4–3.8 5.3–5.9	2.3–3.0 2.4–3.3	60–68 60–69	100 × 002040	12	<0.02 <0.08

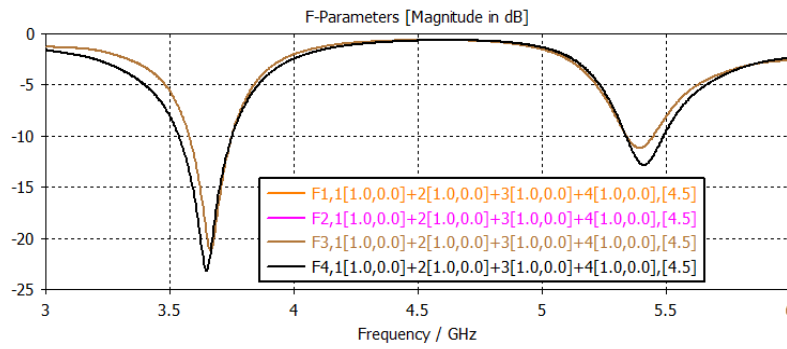


Figure 16: Simulated F-parameter results for the proposed antenna

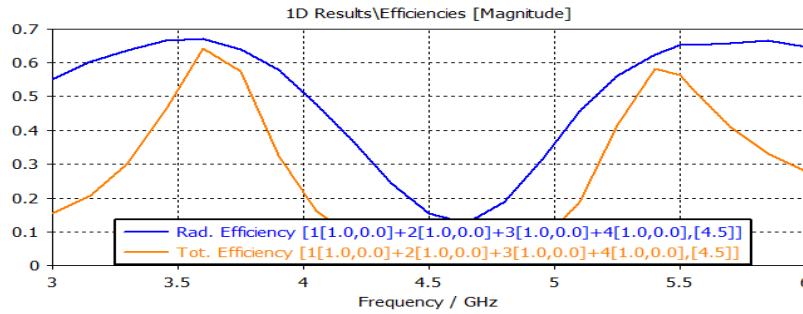


Figure 17: Simulated Radiation and Total Efficiency of Proposed Antenna with Simultaneous Excitation of All Four Ports

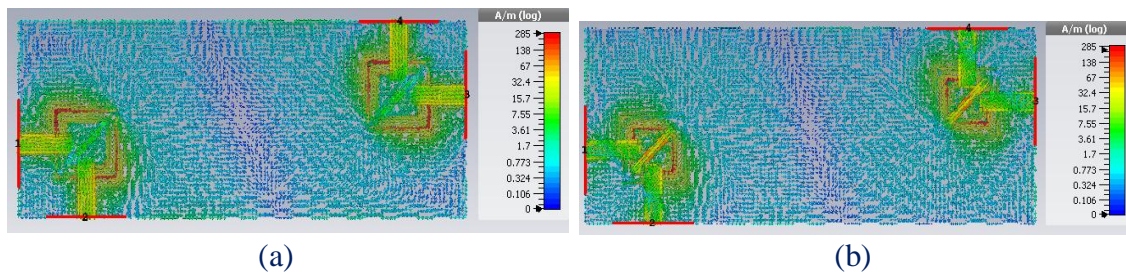


Figure 18: Distribution of Surface Current Vector at (a) 3.6 GHz and (b) 5.5 GHz with simultaneous excitation of all ports of the proposed antenna

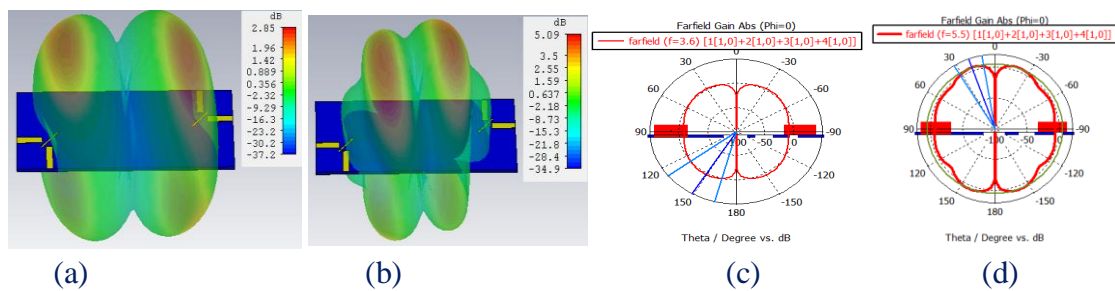


Figure 19: (a) 3D radiation pattern of the proposed antenna at 3.6 GHz (b) 3D radiation pattern of the proposed antenna at 5.5 GHz (c) Polar plot of antenna gain of the proposed antenna at 3.6 GHz (d) Polar plot of the antenna gain of the proposed antenna at 5.5 GHz

All the results mentioned above are for sequential mode excitation of the ports of the antenna. An essential essence for the 5G antenna is beam steering, which is done by exciting the antenna port simultaneously with signals of the same or different phases. S-parameters are no longer valid with

simultaneous excitation, and one has to consider a new set of parameters called F-parameters. The F-parameter results are shown in Figure 16. All the ports are excited with a signal of the same amplitude with zero phase difference.

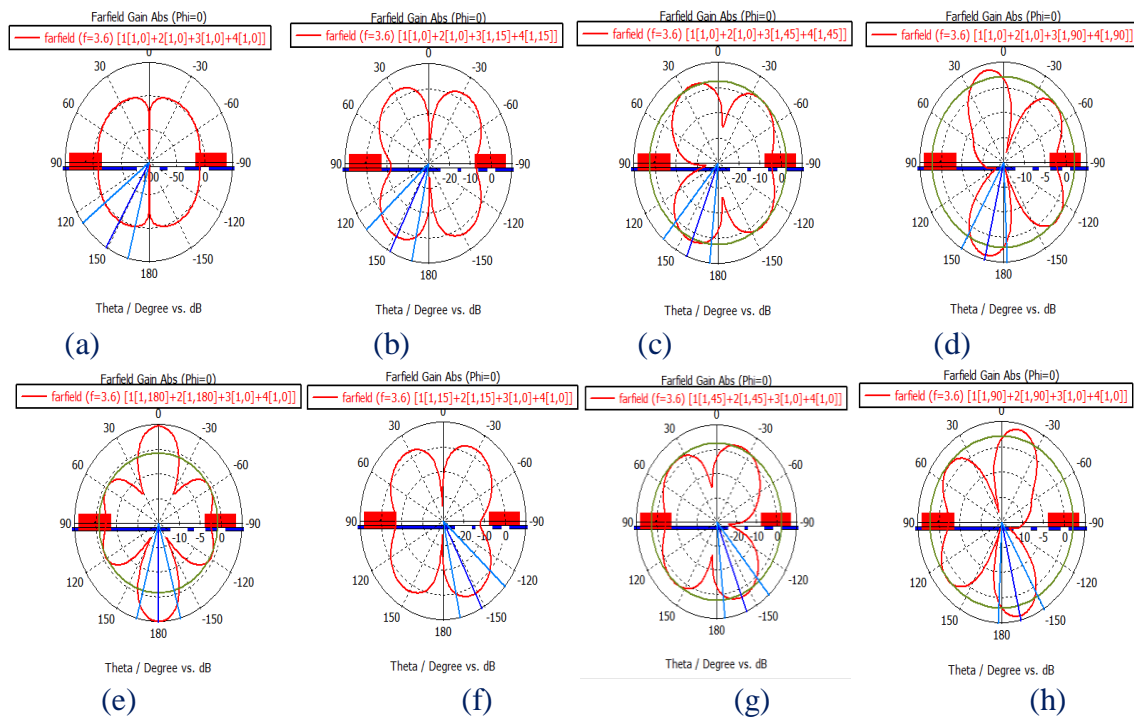


Figure 20: Polar plot of the pattern of the proposed antenna with excitation signal of the same amplitude but different phases at 3.6 GHz

The results obtained during simulation like the plot of radiation efficiency and total efficiency in Figure 17, surface current distribution in Figure 18, radiation pattern with gain for both operating frequencies in Figure 19 are presented for simultaneous excitation signal of equal magnitude and zero phase difference.

4. Conclusions

A dual-band four-port antenna with good gain and efficiency for compact smartphones has been proposed. Double-element slot resonators are used to get dual-band characteristics, and dual-polarization is achieved by exciting the feedlines placed perpendicular to each other. The same antenna can be used with sequential excitation as well as simultaneous excitation with a gain of 3.04 dB at 3.6 GHz and 3.32 dB at 5.5 GHz in sequential mode excitation and 4.84 dB at 3.6 GHz and 5.43 dB at 5.5 GHz in simultaneous mode excitation. The obtained 6dB bandwidth of the antenna is 400 MHz (3.4 - 3.8 GHz) and 600 MHz (5.3 - 5.9 GHz) with

3.6 GHz and 5.5 GHz resonant frequencies, respectively, and covers the desired 5G and WLAN bands. The other parameters like ECC, diversity gain are also well above the specified theoretical values. The experimental results back the simulation results. This antenna is an excellent candidate for a small 5G smartphone in near future.

5. Acknowledgements

I would like to thank Dr. Sanjeev Yadav, Department of ECE, GWECA, for providing me guidance and simulation facilities in his institute. I am grateful to Dr. M. V. Deepak Nair, Assistant Professor, LNMIIT, Jaipur, for providing me the antenna fabrication facilities. Ms. Pooja Bhati, Dr. Ashok Kumar for providing the antenna testing facilities in GWEC Ajmer. I would also acknowledge Mr. Sayyed Arif Ali, Research Scholar, AMU, to perform these simulations and fabrication for his suggestions and support.

References

1. Abdullah, A., Ojaroudi Parchin, N., Abd-Alhameed, R., Noras, J., & Al-Yasir, Y. (2018). A New Polarization-Reconfigurable Antenna for 5G Applications. *Electronics*, 7(11), 293. <https://doi.org/10.3390/electronics7110293>
2. Ge, L., Yang, X., Zhang, D., Li, M., & Wong, H. (2017). Polarization-Reconfigurable Magnetoelectric Dipole Antenna for 5G Wi-Fi. *IEEE Antennas and Wireless Propagation Letters*, 16(c), 1504–1507. <https://doi.org/10.1109/LAWP.2016.2647228>
3. Kahng, S., Khattak, M. K., Khattak, M. S., Rehman, A., Lee, C., Han, D., & Park, H. (2017). Hybrid MIMO antennas for future 5G smartphone applications. 2017 Sixth Asia-Pacific Conference on Antennas and Propagation (APCAP), 1–3. <https://doi.org/10.1109/APCAP.2017.8420795>
4. KHOUMA, M. M., DIOUM, I., SANE, L., DIOP, I., DIALLO, K., & NGOM, A. (2018). Miniature MIMO Antennas for 5G Mobile Terminals. 2018 6th International Conference on Multimedia Computing and Systems (ICMCS), 1–6. <https://doi.org/10.1109/icmcs.2018.8525870>
5. Liu, D., Hong, W., Rappaport, T. S., Luxey, C., & Hong, W. (2017). What will 5G Antennas and Propagation Be? *IEEE Transactions on Antennas and Propagation*, 65(12), 6205–6212. <https://doi.org/10.1109/tap.2017.2774707>
6. Marcus, M. J. (2015). 5G and “IMT for 2020 and beyond” [Spectrum Policy and Regulatory Issues]. *IEEE Wireless Communications*, 22(4), 2–3. <https://doi.org/10.1109/MWC.2015.7224717>
7. Ojaroudi Parchin, N., Jahanbakhsh Basherlou, H., Al-Yasir, Y. I. A., Ullah, A., Abd-Alhameed, R. A., & Noras, J. M. (2019). Multi-Band MIMO Antenna Design with User-Impact Investigation for 4G and 5G Mobile Terminals. *Sensors*, 19(3), 456. <https://doi.org/10.3390/s19030456>
8. Parchin, N. O., Al-Yasir, Y. I. A., Ali, A. H., Elfergani, I., Noras, J. M., Rodriguez, J., & Abd-Alhameed, R. A. (2019). Eight-Element Dual-Polarized MIMO Slot Antenna System for 5G Smartphone Applications. *IEEE Access*, 7, 15612–15622. <https://doi.org/10.1109/ACCESS.2019.2893112>
9. Sarkar, D., & Srivastava, K. V. (2018). Four Element Dual-band Sub-6 GHz 5G MIMO Antenna Using SRR-loaded Slot-Loops. 2018 5th IEEE Uttar Pradesh Section International Conference on Electrical, Electronics and Computer Engineering (UPCON), 1–5. <https://doi.org/10.1109/UPCON.2018.8596789>
10. Saxena, S., Kanaujia, B. K., Dwari, S., Kumar, S., & Tiwari, R. (2018). MIMO antenna with built-in circular shaped isolator for sub-6 GHz 5G applications. *Electronics Letters*, 54(8), 478–480. <https://doi.org/10.1049/el.2017.4514>
11. Vaswani, J., & Agarwal, A. (2020). A Four Port , Dual Band Antenna For Fifth Generation Mobile Communication And WLAN Services. *ACTA TECHNICA CORVINIENSIS – Bulletin of Engineering*, 4(XIII), 73–76. <http://acta.fih.upt.ro/pdf/2020-4/ACTA-2020-4-13.pdf>
12. Vaswani, Jitendra, & Agarwal, A. (2021). Dual-Band, Dual-Polarized Two Element Slot Antenna for Fifth Generation Mobile Devices. *Turkish Journal of Computer and Mathematics Education (TURCOMAT)*, 12(3), 4822–4830. <https://doi.org/10.17762/turcomat.v12i3.1986>
13. Zhu, L., Hwang, H., Ren, E., & Yang, G. (2017). High performance MIMO antenna for 5G wearable devices. 2017 IEEE International Symposium on Antennas and Propagation & USNC/URSI National Radio Science Meeting, 2017-Janua, 1869–1870. <https://doi.org/10.1109/APUSNCURSINRSM.2017.8072977>